Electron Transfer Reactions in Zn-Substituted Cytochrome P450cam†

Yoshiaki Furukawa, Koichiro Ishimori, and Isao Morishima*

Department of Molecular Engineering, Graduate School of Engineering, Kyoto University, Kyoto 606-8501, Japan

Received April 18, 2000; Revised Manuscript Received June 19, 2000

ABSTRACT: We have investigated photoinduced electron transfer (ET) reactions between zinc-substituted cytochrome P450cam (ZnP450) and several inorganic reagents by using the laser flash photolysis method, to reveal roles of the electrostatic interactions in the regulation of the ET reactions. The laser pulse irradiation to ZnP450 yielded a strong reductant, the triplet excited state of ZnP450, ^{3}ZnP450*, which was able to transfer one electron to anionic redox partners, $OsCl_6^{2-}$ and $Fe(CN)_6^{3-}$, with formation of the porphyrin π-cation radical, $ZnP450^+$. In contrast, the ET reactions from ^{3}ZnP450* to cationic redox partners, such as $Ru(NH_3)_6^{3+}$ and $Co(phen)_3^{3+}$, were not observed even in the presence of 100-fold excess of the oxidant. One of the possible interpretations for the preferential ET to the anionic redox partner is that the cationic patch on the P450cam surface, a putative interaction site for the anionic reagents, is located near the heme (less than 10 Å from the heme edge), while the anionic surface is far from the heme moiety (more than 16 Å from the heme edge), which would yield 8000-fold faster ET rates through the cationic patch. The ET rate through the anionic patch to the cationic partner would be substantially slower than that of the phosphorescence process in ^{3}ZnP450*, resulting in no ET reactions to the cationic reagents. These results demonstrate that the asymmetrical charge distribution on the protein surface is critical for the ET reaction in P450cam.

Cytochrome P450cam (P450cam) from *Pseudomonas putida* is one of the hemoproteins for the electron transfer (ET) reactions, which catalyzes the regio- and stereospecific hydroxylation of its substrate, *d*-camphor, at the 5-*exo* position (*1*). The reaction cycle requires two electrons, which are sequentially transferred by a [2Fe-2S] cluster protein, putidaredoxin (Pd), from Pd reductase to P450cam. As studied intensively by many investigators (*2*−*6*), electrostatic interactions between P450cam and Pd have an important role in the protein−protein recognition for the efficient ET reaction. Some amino acid residues on the protein surface have been mutated to characterize the electrostatic interactions. For example, Holden et al. (*5*) have reported that neutralization of the positive charge at Asp38 on Pd resulted in ca. 20-fold increase of the dissociation constant to P450cam and the decreased ET rate. In P450cam, mutations to neutralize the basic residues near the active site (Arg112) also enhanced the dissociation of the ET complex with Pd and depressed the ET process (*4*).

In addition to the mutational studies, the computer simulations have demonstrated the importance of the electrostatic interactions in the P450cam/Pd association (*3*, *7*, *8*). As suggested by Stayton and Sligar (*3*), the electrostatic modeling on P450cam would provide a visualized rationale for effects of the surface charge on the association with Pd. The surface of P450cam is dominated by anionic potential with the largest continuous cationic patch lying on the nearest proximal approach to the buried heme prosthetic group (Figure 1). On the other hand, the protein surface of Pd is negatively charged by anionic residues, resulting in an effective steering to the more electrostatically favorable cationic patches on P450cam.

However, it is also plausible that the mutation for the charge neutralization often affects other interactions between P450cam and Pd such as van der Waals contacts and hydrophobic interactions, which complicates the interpretation of the mutational effects and computer simulation. To simplify the ET reaction system and enhance the effects of electrostatic interaction on the ET reaction, many studies have utilized small inorganic reagents as models for its physiological partner proteins (*9*−*11*). By using small and isostructural inorganic compounds as redox partners, the steric and hydrophobic effects can be regulated. Such approaches have been applied to the ET reaction of blue copper protein (*11*, *12*), cytochrome (*10*, *13*), and iron−sulfur proteins (*9*, *14*), by which some interaction sites for the ET reactions have been identified and the ET processes have been characterized.

In this study, we examined the ET reactions between Zn-substituted P450cam (ZnP450) and anionic/cationic inorganic reagents to elucidate the roles of electrostatic interactions on the ET reactions. As previously reported (*15*, *16*), replacement of Fe(II) by Zn(II) does not perturb the conformation of many 5-coordinated hemoproteins, and the triplet-excited state of zinc-porphyrin is long-lived and suitable for various kinetic studies. In the thermodynamic respect, the triplet-excited state of ZnP450 (^{3}ZnP450*) is a strong reductant, which can readily transfer one electron to

† This work was supported by a grant from Ministry of Education, Science, Culture, and Sports (no. 08249102 to I.M. and K.I.).

* To whom correspondence should be addressed at the Department of Molecular Engineering, Graduate School of Engineering, Kyoto University, Kyoto 606-8501, Japan. Phone: +81-75-753-5921. Fax: +81-75-751-7611. E-mail: morisima@mds.moleng.kyoto-u.ac.jp.

10.1021/bi000874y CCC: $19.00
Published on Web 08/18/2000

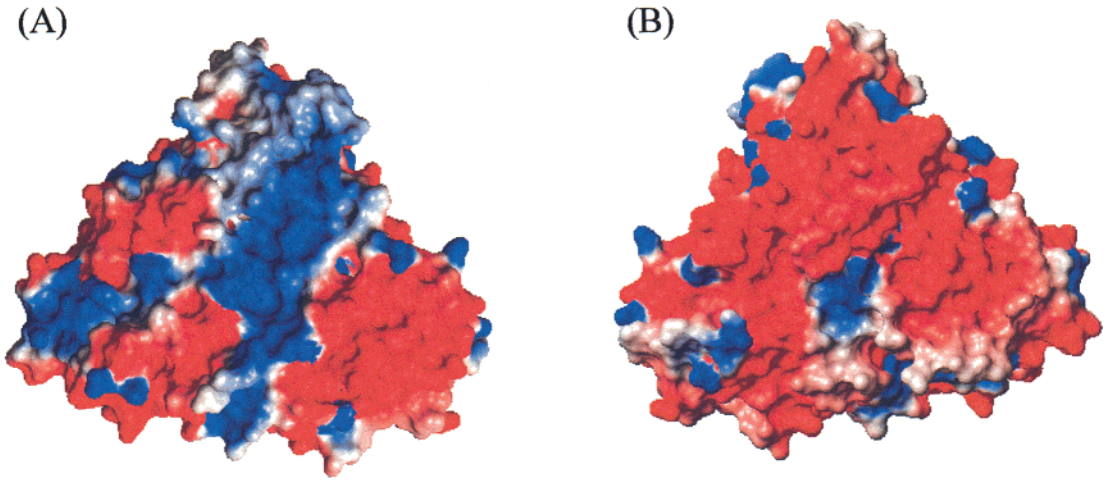

FIGURE 1: Electrostatic surface of P450cam calculated by the MOLMOL program at an ionic strength of 150 mM. The positively charged surface is colored blue, while the negatively charged one is red. Data are taken from the 2.6 Å resolution crystal structure (ref *25*). (A) The proximal surface. (B) The distal surface.

various inorganic reagents due to the large redox potential difference.

As electron acceptors, we have used the following negatively or positively charged inorganic oxidants: $OsCl_6^{2-}$, $Fe(CN)_6^{3-}$, $Co(phen)_3^{3+}$, and $Ru(NH_3)_6^{3+}$. In the presence of one of these redox reagents, laser irradiation to ZnP450 can promote the ET reaction from ZnP450 to the redox reagent, when ZnP450 can interact with the reagent to form the complex. In terms of the electrostatic interactions, anionic compounds, $OsCl_6^{2-}$ and $Fe(CN)_6^{3-}$, would preferentially react at the basic patch on the P450cam surface, whereas cationic $Co(phen)_3^{3+}$ and $Ru(NH_6)_6^{3+}$ would have primary interactions with the dominated anionic surface on P450cam. These small inorganic reagents are almost isostructural, which enables us to evaluate the electrostatic interactions between the charges on the protein surface of P450cam and on the inorganic reagents. Another advantageous point is that, unlike the P450cam/Pd complex, the distance between the donor and acceptor in the P450cam−inorganic reagent complex can be readily estimated and we can apply the Marcus theory to the ET reaction. The application of the Marcus theory would provide us with various theoretical aspects for the ET reactions.

EXPERIMENTAL PROCEDURES

Preparation of Zn-Substituted Cytochrome P450cam. P450cam was prepared as described elsewhere (*17*). The finally purified P450cam gave a single band on SDS−polyacrylamide gels, and the A_{391}/A_{280} ratio was more than 1.4. The apo-form of P450cam was prepared by the acid−butanone procedure of Wagner et al. (*18*). P450cam was dissolved in 0.1 M histidine solution (pH 7.8), and the pH of the protein solution (ca. 15 mL) was lowered to 2.7 on ice. To extract the heme, an equivolume of 2-butanone was added to the solution. The extraction was repeated twice, and the aqueous apoprotein solution was dialyzed against 2 L of 0.6 mM $NaHCO_3$ overnight. Apoprotein was subsequently dialyzed against 2 L of 0.1 M histidine containing 40% (v/v) glycerol overnight. Then, the apoprotein solution (ca. 50 mL) was degassed and purged with purified argon gas, followed by incubation with 10 mM dithiothreitol (DTT) at room temperature for an hour under an argon atmosphere. An equivolume of degassed 0.1 M histidine, pH 8.0, and 5% (v/v) of aqueous saturated *d*-camphor (ca. 5 mL) was added to the protein solution. A stoichiometric amount of Zn-protoporphyrin IX diacid, ~5 mg, was dissolved in 0.5 mL of dimethylformamide, and added dropwise to the magnetically stirred solution of apoprotein. Reconstitution was performed under an argon atmosphere for 48 h at room temperature.

The crude ZnP450 was purified by a HiTrapQ anion-exchange column for the Pharmacia FPLC system. The sample was loaded on the column in 40 mM potassium phosphate/1 mM *d*-camphor, pH 8.0, and eluted with a linear gradient of 40 mM potassium phosphate/1 mM *d*-camphor/400 mM KCl, pH 8.0. Sample purity was checked by SDS−PAGE. All manipulations of ZnP450 were performed in the dark.

The extinction coefficient of ZnP450 at pH 7.0 was determined by ICP emission spectroscopy (Jarrel Ash ICAP-500). The emission of zinc ion excited by argon plasma was measured at 213.86 nm, and zinc standard solution (1, 2, 3 ppm) (Wako) was used for the calibration line.

Spectroscopic Methods. The UV/vis spectra were obtained by using a Perkin-Elmer Lambda 18 spectrophotometer at room temperature in 40 mM potassium phosphate buffer with 1 mM *d*-camphor at pH 8.0.

Circular dichroism (CD) spectra of P450cam and ZnP450 were measured in 40 mM potassium phosphate buffer with 1 mM *d*-camphor at pH 8.0 using Jasco J-720. The path length of the cell was 1 mm, and the protein concentration was ca. 5 μM. All CD spectra in this paper were an average of 10 scans recorded at a speed of 200 nm/min and a resolution of 0.2 nm. The α-helix contents of proteins are calculated from the ellipticities at 222 nm by utilizing the equation (*19*):

$$f_H = -\frac{[\theta]_{222} + 2340}{30\,300} \quad (1)$$

where f_H is the α-helix content and $[\theta]_{222}$ is the mean residue ellipticity at 222 nm.

EPR spectra of ZnP450 were measured by a Varian E-12 spectrometer equipped with an Oxford ESR-900 liquid

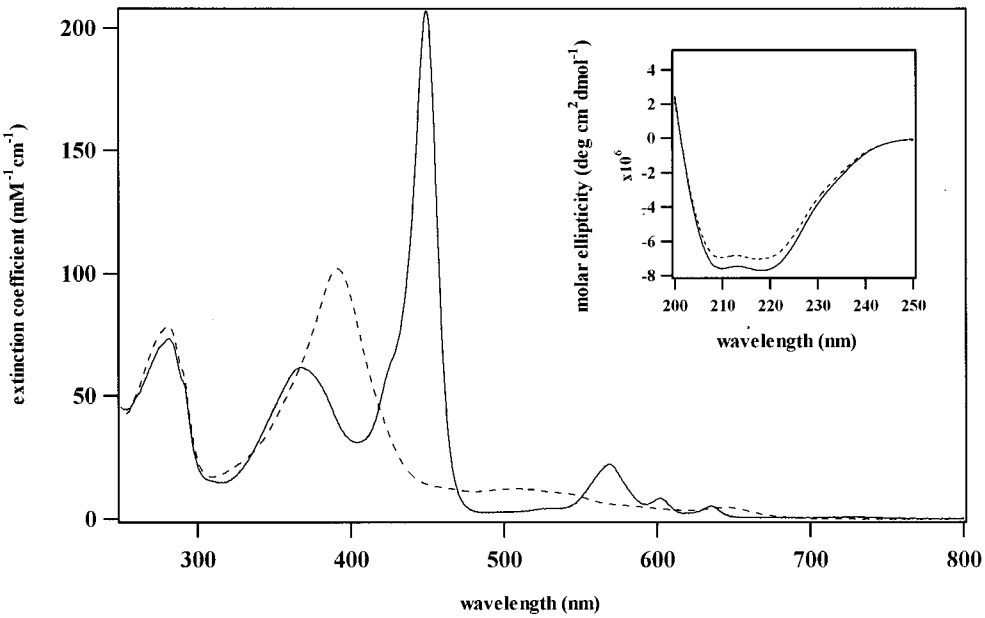

FIGURE 2: Electronic absorption spectra of ZnP450 (solid curve) and ferric P450cam (dashed curve) in 40 mM K-P_i, 1 mM *d*-camphor, pH 8.0, at room temperature. (Inset) Circular dichroism spectra of ferric P450cam (dashed curve) and ZnP450 (solid curve) in the far-UV region. Conditions: 40 mM K-P_i, 1 mM *d*-camphor, pH 8.0, at room temperature.

helium cryostat. Measurements were carried out at the X-band (9.22 GHz) microwave frequency at 35 K. The microwave power was 0.1 mW. The concentration of ZnP450 was ca. 200 μM, and the sample volume was 20 μL. To observe the EPR signal from the ZnP450 π-cation radical, the rapid mixing and freezing method was utilized. The small excess K_2IrCl_6 (ca. 200 μM, 20 μL) and ZnP450 were set in the bottom and middle of the EPR tube, respectively. After shaking the EPR tube to mix the solutions, it was frozen in liquid nitrogen within 10 s.

Stopped-Flow Experiment. The oxidation of ZnP450 by K_2IrCl_6 was observed with a rapid-scanning monochromator (OLIS) equipped with a stopped-flow spectrophotometer (UNISOKU). The buffer system used in this experiment was 40 mM potassium phosphate/1 mM *d*-camphor, pH 8.0, and the reactions were carried out at 4 °C controlled by a circulating methanol bath. Since K_2IrCl_6 is known to be unstable at high pH, its stock solution was weakly acidified with HCl.

Flash Photolysis Measurement. The transient difference spectra after the irradiation of a laser pulse were measured with the double flash system developed by Orii (*20*). The second harmonic (532 nm) of a Q-switched Nd:YAG laser provides photolysis pulses with a half-peak duration of 10 ns. The monitoring beam was generated by a xenon lamp (150 W), and focused on the sample cell at the right angle of the excitation source. The transmitted light was detected by a photomultiplier that is attached on a monochromator, UNISOKU USP-501. A two-channel oscilloscope (TDS 500) was used to digitize and accumulate the signals that were transferred to a NEC PC-98 computer for further analysis. Temperature was controlled by using a circulating water bath (±0.1 °C).

Reaction Mechanism. A general mechanism for the ET reactions between two molecules, A and D, is shown as below (*21*). k_{on} and k_{off} show the rate constants for the association and the dissociation process, respectively, and k_{ET} is the ET rate constant in the complex formed by the two reactant molecules, A and D.

$$D + A \underset{k_{off}}{\overset{k_{on}}{\rightleftharpoons}} DA \xrightarrow{k_{ET}}$$

Under the steady-state approximation and the condition [A] ≫ [D], eq 2 is obtained. When $k_{off} \gg k_{on}[A] + k_{ET}$, eq 2 can be simplified to eq 3, where the association constant K_A equals k_{on}/k_{off}.

$$k_{obs} = \frac{k_{ET}k_{on}[A]}{k_{on}[A] + k_{off} + k_{ET}} \quad (2)$$

$$k_{obs} = K_A k_{ET}[A] = k[A] \quad (3)$$

Table 1: Absorption Maxima of Various Zinc-Substituted Hemoproteins

	nm (mM^{-1} cm^{-1})			
	hyper	Soret	β	α
ZnP450	367 (65.4)[f]	449 (207)	568 (23.6)	602 (9.3)
Zn-myoglobin[a]	ND[b]	428	553	595
Zn-cytochrome *c*[c]	346	423	549	584
ZnTPP + SBu^- [d]	378	449	587	633
ZnTPP + ImH[e]	ND[b]	431	566	606

[a] Ref *22*. [b] Not detected. [c] Ref *23*. [d] Zn-tetraphenylporphyrin complexed with butyl thiolate (*24*). [e] Zn-tetraphenylporphyrin with imidazole (*24*). [f] The values in parentheses show the molar extinction coefficient at each wavelength.

RESULTS

Spectroscopic Characterization of ZnP450. Figure 2 shows the electronic absorption spectrum of ZnP450 (solid line). Unlike histidine-ligated Zn-porphyrin-substituted hemoproteins such as zinc-myoglobin (*22*) or zinc-cytochrome *c* (*23*), the Soret band of ZnP450 was abnormally red-shifted to 449 nm, and a so-called "hyper band" (the absorption around 350 nm) was observed (Table 1). The "hyper band" was also found for a complex of Zn-tetraphenylporphyrin (ZnTPP)

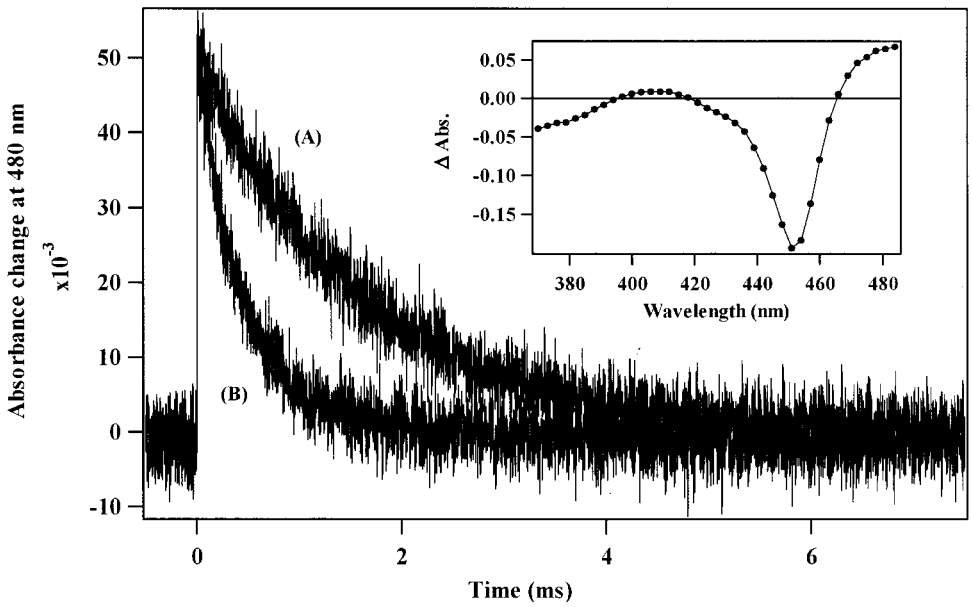

FIGURE 3: Transient absorbance changes at 480 nm obtained after laser excitation of (A) ZnP450 and (B) in the mixture of ZnP450 and $Fe(CN)_6^{3-}$. The sample solution contains 2 μM ZnP450 and 40 μM $Fe(CN)_6^{3-}$ in 40 mM K-P_i, 1 mM *d*-camphor, pH 7.4 at 293 K. (Inset) Transient difference spectra between ^{3}ZnP450* and ZnP450 after a laser shot.

with cysteine (*24*) (Table 1), indicative of sulfur ligation to the Zn-porphyrins. The unusual red-shift of the Soret peak of ZnP450 is another evidence for the cysteine ligation to ZnP in ZnP450. The butyl thiolate-ligated ZnTPP (*24*) has the Soret peak at 449 nm, which is red-shifted from that in imidazole-ligated ZnTPP (431 nm) (Table 1).

To confirm that the metal substitution in P450cam does not perturb the protein structure, we measured the CD spectra of ZnP450. In the inset of Figure 2, the CD spectra of ZnP450 (solid curve) and P450cam (dashed curve) in the far-UV region are shown. The α-helical content, calculated from the molar ellipticities at 222 nm by using eq 1, was 45% and 50% for P450cam and ZnP450, respectively. These values are in good agreement with that estimated from the X-ray crystal structure (53%) (*25*). The Zn substitution in P450cam does not, therefore, perturb the protein secondary structure.

Generation and Decay of the Triplet-Excited State of ZnP450. Generation of the triplet-excited state of ZnP450, ^{3}ZnP450*, as the reductant for the ET reaction in this system, was evident by comparison of the transient difference spectrum before and immediately after the laser illumination under anaerobic conditions (inset of Figure 3). Flash illumination of ZnP450 yields the bleaching of the Soret band and the increase of the absorbance around 480 nm. This spectral change is characteristic of the transition from the ground state to the triplet-excited state of the Zn-substituted hemoprotein (*26*). The transient absorbance change at 480 nm, where ^{3}ZnP450* mainly absorbs, is shown in Figure 3(A). By fitting a single-exponential function, the triplet decay rate constant, 6.2×10^2 s^{-1} at 293 K, was obtained. Random residuals from a single-exponential fitting (data not shown) indicate that the decay of the triplet state in ZnP450 is monophasic. The triplet decay rate was not dependent on the sample concentration, showing the absence of bimolecular quenching of ^{3}ZnP450*. The equilibrium spectra of ZnP450 were virtually the same before and after laser irradiation, which ensures that ZnP450 was not degradated throughout the laser experiment.[1]

Table 2: Ground-State and Excited-State Reduction Potentials in Zn-Substituted Hemoproteins

proteins	$E(ZnP^+/ZnP)$,[a] eV	$E(ZnP^+/^3ZnP^*)$,[b] eV
Zn-myoglobin[c]	0.98	−0.80
Zn-hemoglobin[d]	1.2	−0.62
Zn-cytochrome *c*[e]	0.80	−1.1
ZnP450	1.0[f]	−0.9[f]

[a] The reduction potential of porphyrin π-cation radical in Zn-substituted hemoproteins. [b] The redox potential between porphyrin π-cation radical and triplet-excited state in Zn-substituted hemoproteins. [c] Ref *26*. [d] Ref *28*. [e] Ref *27*. [f] Estimated values by using the other data as mentioned in the text.

Redox Potential of ZnP450. In addition to the generation of ^{3}ZnP450*, higher redox potential of ^{3}ZnP450* than that of the redox partner is required for the ET reaction. The $ZnP450^+/^3ZnP450^*$ reduction potential is defined as follows:

$$E(ZnP450^+/^3ZnP450^*) = E(ZnP450^+/ZnP450) - E(^3ZnP450^*) \quad (4)$$

where $E(^3ZnP450^*)$ is the excited-triplet energy and $E(ZnP450^+/ZnP450)$ is the ground-state reduction potential. $E(^3ZnP450^*)$ can be determined from the phosphorescence spectrum of ZnP450 at ambient temperature (*27*). The phosphorescence peak was observed around 640 nm (data not shown), corresponding to 1.9 eV as $E(^3ZnP450^*)$. Although the instability of $ZnP450^+$ prevents us from estimating $E(ZnP450^+/ZnP450)$, the reduction potential for Zn-porphyrin π-cation radical is reported to be approximately 1.0 eV in some Zn-substituted hemoproteins (*27*−*29*) (Table 2). It is, therefore, plausible that $E(ZnP450^+/^3ZnP450^*)$ is about −0.9 eV. The estimated $E(ZnP450^+/^3ZnP450^*)$ is

[1] When the sample contains dissolved oxygen, the intensity of the absorption peak at 635 nm was increased and the Soret band was bleached upon illumination. Extraction of the chromophore from the illuminated ZnP450 using the acidic 2-butanone method gave a chlorin-like absorption spectrum. The illumination of ZnP450 under aerobic conditions degradates the porphyrin ring of ZnP.

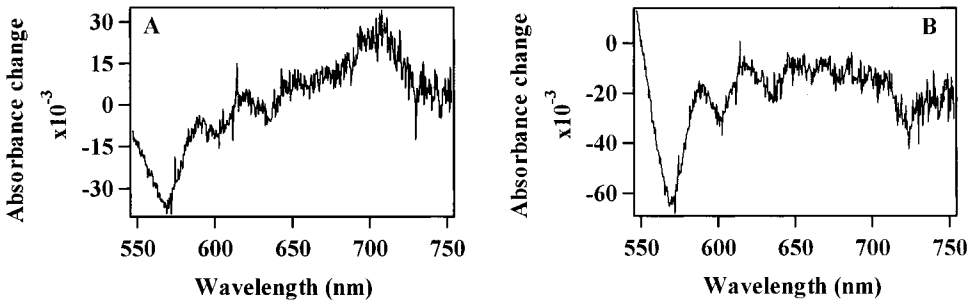

FIGURE 4: Transient difference absorbance spectrum of 2 μM ZnP450 (A) in the presence of excess $Fe(CN)_6^{3-}$ and (B) in the absence of $Fe(CN)_6^{3-}$ after the laser pulse.

Table 3: Thermodynamic Parameters of the Inorganic Quenchers Used in This Study

redox partners	ΔG^o, eV	a, Å	λ_{22}, eV	λ, eV	relative value of nuclear factor
$OsCl_6^{2-}$	+0.45[a]	2.2[b]	1.8	1.5	1.1
$Fe(CN)_6^{3-}$	+0.36[c]	4.5[c]	0.9	1.1	1.0
$Co(phen)_3^{3+}$	+0.37[d]	7.0[d]	0.7	1.0	0.6
$Ru(NH_3)_6^{3+}$	+0.07[d]	3.3[d]	1.2	1.2	0.8

[a] Ref *38*. [b] The ionic radius of $OsCl_6^{2-}$ is not available. We estimated it based on the data of $IrCl_6^{2-}$ (38), which is analogous to $OsCl_6^{2-}$. [c] Ref *37*. [d] Ref *36*.

comparable to previously reported values for Zn-substituted hemoproteins as summarized in Table 2, indicating that ^{3}ZnP450* can reduce the inorganic reagents in this study (Table 3) and Pd ($E^\circ = -0.2$ eV).

ET Reactions of ZnP450 with Inorganic Reagents. As previously reported (*30*), in the presence of some redox partners, ^{3}ZnP450* can transfer one electron to the redox partner, which accelerates the decay of the triplet state. Figure 3 represents the time course of the absorbance change at 480 nm, and the decay was accelerated by addition of the anionic redox partner $Fe(CN)_6^{3-}$. The kinetic trace can be fitted by a single-exponential function with random residuals (data not shown), indicating that the decay of ^{3}ZnP450* is monophasic and the rate was 8.8×10^3 s^{-1}.

Although the acceleration of the decay is indicative of the ET reaction from ^{3}ZnP450* to the anionic redox partner, the energy transfer can also accelerate the decay of ^{3}ZnP450* (*31*). To confirm the ET reaction, we measured the transient absorption spectrum of the reaction. In the ET reaction from ^{3}ZnP450* to the redox partner, the zinc porphyrin π-cation radical is formed as the reactive intermediate, whose absorption spectrum is characterized by the broad peak around 700 nm. The difference spectrum obtained after subtraction of the spectrum before the laser irradiation from that immediately after the irradiation (about 100 ms) (Figure 4) exhibits the significant increase of the absorbance around 700 nm, showing the formation of $ZnP450^+$ in the reaction.

To further characterize the reaction intermediate in the reaction, we determined the oxidation state by the reaction with the one-electron oxidant K_2IrCl_6 (*32*, *33*). Upon addition of K_2IrCl_6, prominent new bands appeared at 705.5 and 360 nm (Figure 5) as found for the transient spectrum in the reaction of ^{3}ZnP450* with the redox partner. The isosbestic points were clearly seen at 407 and 468 nm during the spectral transition. The maximum change of the absorption at 705.5 nm was plotted against the K_2IrCl_6 concentration (inset of Figure 5). As clearly shown in the inset, equimolar

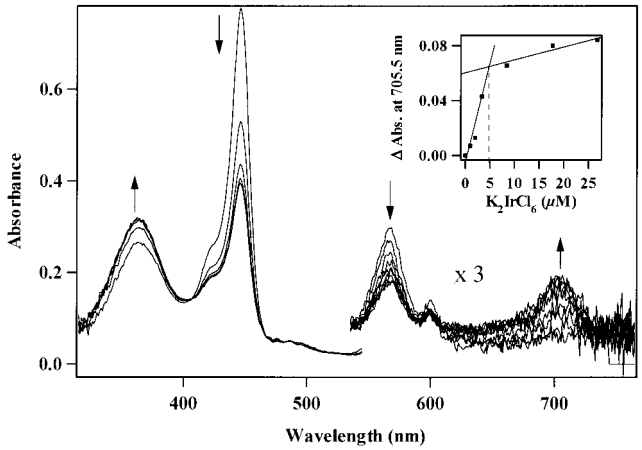

FIGURE 5: Rapid spectral scanning experiments for 8.8 μM ZnP450 after addition of 20 μM K_2IrCl_6. The scans were recorded at 130, 150, 170, 190, and 210 ms after addition of K_2IrCl_6. (Inset) Absorbance changes at 705.5 nm immediately after addition of K_2IrCl_6 are plotted against the concentration of K_2IrCl_6. The condition is 4.4 μM Zn450 in 40 mM K-P_i, 1 mM *d*-camphor, pH 8.0, at 277 K.

K_2IrCl_6 was required to complete the oxidation of ZnP450, indicating that the oxidation state of oxidized ZnP450 is 1 equiv higher than that before addition of K_2IrCl_6. Since the Zn ion cannot be oxidized from Zn(II) to Zn(III) and the oxidized aromatic residues such as Tyr and Trp radicals do not have an absorption around 700 nm, these spectral changes of ZnP450 support the formation of a porphyrin π-cation radical.

The ESR spectrum of oxidized ZnP450 provided us with additional evidence for the π-cation radical on the porphyrin ring. An EPR signal appeared at $g = 2.0026$ upon addition of K_2IrCl_6 (Figure 6), and the g value of K_2IrCl_6-oxidized ZnP450 is similar to those of Zn-octaethylporphyrin oxidized by ferric perchlorate ($g = 2.0025$) (*34*) and porphyrin π-cation radical in Zn-HRP (*33*).[2] Thus, these spectral changes unambiguously indicate that the acceleration of the decay of ^{3}ZnP450* by addition of $Fe(CN)_6^{3-}$ is ascribed to the ET from ^{3}ZnP450* to $Fe(CN)_6^{3-}$, not to the energy transfer. Acceleration of the decay with similar spectral changes to those by addition of $Fe(CN)_6^{3-}$ was also encountered in the presence of another anionic redox partner, $OsCl_6^{2-}$. Although the quantitative analysis of the reaction of ^{3}ZnP450* with $OsCl_6^{2-}$ has yet not been successful due to the uncertainty of the absorption coefficients of $OsCl_6^{2-}$, the ET from ^{3}ZnP450* to another anionic redox partner, $OsCl_6^{3-}$, was also induced.

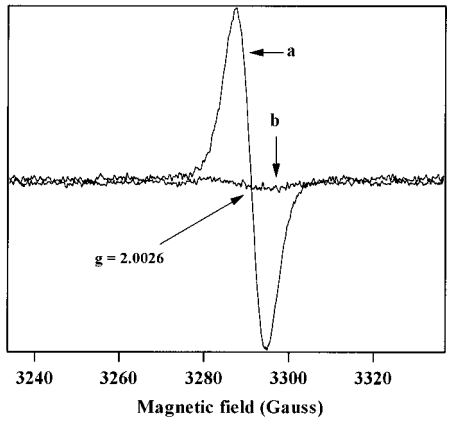

FIGURE 6: ESR spectrum obtained by rapidly mixing ZnP450 (20 μL, 192 μM) and K_2IrCl_6 (18 μL, 213 μM) and freezing its mixture in liquid nitrogen within 10 s (curve a). Curve b is ZnP450 without K_2IrCl_6.

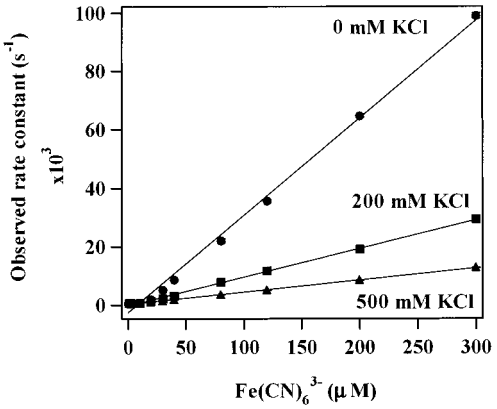

FIGURE 7: Dependence of the quenching rate constant of ^{3}ZnP450* upon $Fe(CN)_6^{3-}$ concentration in a solution containing 0, 200, and 500 mM KCl. Conditions: 2 μM ZnP450 in 40 mM K-P_i, 1 mM *d*-camphor, pH 7.4, at 293 K. The line is the least-squares fitting to the data.

In the case of cationic reagents, $Co(phen)_3^{3+}$ and $Ru(NH_3)_6^{3+}$, however, neither formation of ZnP450$^+$ nor acceleration of the ^{3}ZnP450* decay was observed even in the presence of a 100-fold excess (data not shown). The preferential ET reactions to the anionic regents strongly suggest that the interaction responsible for the ET complex is dominated by electrostatic interactions. We examined the electrostatic interactions on the ET reactions between ZnP450 and $Fe(CN)_6^{3-}$ by varying the ionic strength of the solution. As Figure 7 shows, by increasing the KCl concentration, the apparent rate constant for the decay of ^{3}ZnP450* was depressed, and the bimolecular ET rate constants are 3.2×10^8, 9.3×10^7, and 3.9×10^7 M^{-1} s^{-1} under 0, 200, and 500 mM KCl concentration, respectively. The bimolecular ET rate constants were decreased by the increase in the ionic strength in the solution, which supports that ^{3}ZnP450* reacts with $Fe(CN)_6^{3-}$ through electrostatic interactions to transfer an electron.

[2] The UV/vis spectrum of ZnP450$^+$ returned back to that of the original state, ZnP450, within ca. 10 min concomitant with decreasing the intensity of the ESR. These spectral changes were also observed for the oxidation reaction of Zn-hemoglobin, in which the radical transfer to some aromatic residues has been suggested (*28*). The radical transfer to aromatic residues is also possible in ZnP450$^+$, but its detailed mechanism needs further investigations.

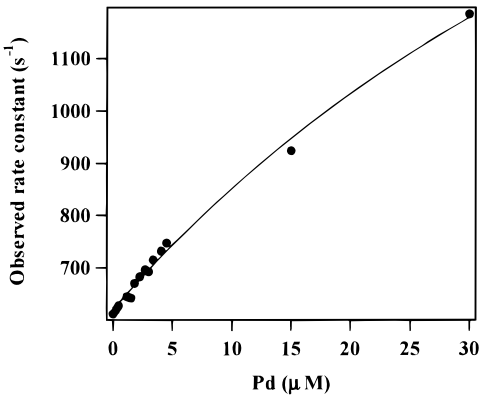

FIGURE 8: Dependence of the quenching rate constant of ^{3}ZnP450* upon Pd^{ox} concentration. The line is the least-squares fitting to the data by using eq 2 (see Results). Conditions: 2.5 μM ZnP450 in 40 mM K-P_i, 1 mM *d*-camphor, pH 7.4, at 293 K.

ET Reactions of ZnP450 with Pd. Under physiological conditions, P450cam was provided electrons from an iron−sulfur protein, Pd, to catalyze the monooxygenation of *d*-camphor (*1*). Since the protein surface of Pd is negatively charged (*35*), the ET reaction from ^{3}ZnP450* to oxidized Pd (Pd^{ox}) was supposed to readily proceed. Although the decay rate of ^{3}ZnP450* was accelerated upon addition of Pd^{ox} (Figure 8), the transient difference spectrum (350 to ~750 nm) between before and after the laser shot was insensitive to addition of Pd^{ox} as shown in Figure 4B. No transient absorbance changes at 705.5 nm, where ZnP450$^+$ mainly absorbs, were observed even with 10-fold excess of Pd^{ox} against ZnP450. The decay was also accelerated by addition of reduced Pd(Pd^{red}). It is evident that no electron was transferred from ^{3}ZnP450* to Pd^{ox}.

The acceleration of the decay of ^{3}ZnP450* is, therefore, due to some energy transfer processes between ^{3}ZnP450* and Pd^{ox}.[3] Since the decay rate constant of ^{3}ZnP450* is dependent on the Pd^{ox} concentration and shows saturation (Figure 8), the plots were fitted to eq 2, and the apparent association constant between ^{3}ZnP450* and Pd^{ox}, K_A ($=k_{on}/k_{off}$) $= 1.76 \times 10^{-2}$ μM^{-1}, was obtained. Thus, ^{3}ZnP450* can interact with Pd^{ox}, but an electron cannot be transferred to Pd^{ox}.

DISCUSSION

ET Reactions with Inorganic Reagents. To quantitatively analyze the ET process between ZnP450 and the redox partners, we utilized the Marcus theory. In the Marcus theory (*36*), apparent rate constant for the bimolecular ET reactions, k, can be described by the association constant for the ET complex, K_A, and the ET rate constant in the ET complex, k_{ET}, as follows:

$$k = K_A k_{ET}$$

$$= K_A \cdot A \cdot \exp[-\beta(d-3)] \cdot \exp\left[-\frac{(\Delta G^\circ + \lambda)^2}{4\lambda RT}\right] \qquad (5)$$

where A is the constant and β is the distance decay factor.

[3] The aromatic amino acid residue, Trp106, of Pd is positioned at the interface of the physiological P450cam/Pd complex (*7*), and it is required for the efficient ET from Pd to P450cam (*39*). The extended π-electron system at Trp106 of Pd could also serve as a mediator of energy transfer from ^{3}ZnP450* to Pd.

k_{ET} is further composed of the "electronic factor", $\exp[-\beta(d-3)]$, and the "nuclear factor", $\exp[-(\Delta G^\circ + \lambda)^2/4\lambda RT]$.

Since the observed rate constant, k_{obs}, is correlated with k_{ET} by eq 2 under the steady-state approximation, the acceleration of k_{obs} is saturated in the presence of a large excess of [A] and k_{obs} approaches k_{ET} under the condition of $k_{off} + k_{ET} \ll k_{on}[A]$. However, k_{obs} was linearly accelerated by increasing the concentration of the inorganic redox partner even in the presence of a 100-fold excess. These nonsaturation kinetics can be attributed to the large dissociation constant of the inorganic acceptor from ZnP450, i.e., $k_{off} \gg k_{ET} + k_{on}[A]$, leading to eq 3. In eq 3, the ET rate constant in the complex, k_{ET}, cannot be extracted from the observed rate constant, k_{obs}.

Although it is also difficult to estimate the contribution of the association (K_A) to the observed rate constant, k_{obs}, previous studies have reported that the association affinity of protein with small inorganic compounds depends on the net charges of the small molecules and surface charges of the protein (*10*, *36*, *37*). The net charge of the inorganic compound we used here is 2 or 3, and P450cam has both a positively and a negatively charged protein surface, suggesting that the association affinity of ZnP450 with the anionic acceptor is almost the same as that of the cationic acceptor in the present experiments. It is, therefore, likely that the preferential ET reaction from ZnP450 to the anionic donors reflects the difference of k_{ET} between the anionic and cationic redox partners, rather than that of the association affinity with ZnP450, K_A.

In the Marcus equation (eq 5), k_{ET} consists of two factors, nuclear and electronic factors. To evaluate the effects of the nuclear factor on the present ET reactions, we estimated the total reorganization energy, λ. The total reorganization energy, λ, can be divided into the reorganization energy for the self-exchange reactions in ZnP450 (λ_{11}) and the inorganic reagents (λ_{22}) as eq 6 (*36*).

$$\lambda = \frac{\lambda_{11} + \lambda_{22}}{2} \tag{6}$$

λ_{22} can be simply estimated from the ionic radius (a, Å) of the inorganic complexes as follows (*36*):

$$\lambda_{22}(\text{eV}) = \frac{7.20}{a} \times \left(\frac{1}{n^2} - \frac{1}{D}\right) \tag{7}$$

where n is the refractive index of water (1.33) and D is the relative dielectric constant of water (78.5). Table 3 summarizes the ionic radius, a, of the reagents and the calculated reorganization energies (λ_{22}) (*36*−*38*). Although λ_{11} for ZnP450 has not yet been estimated in this experiment, many studies (*30*) have suggested that λ_{11} of Zn-substituted hemoproteins is ca. 1.2 eV. The calculated total reorganization energy is summarized in Table 3.

Another factor affecting the nuclear factor is the free energy difference, ΔG°, which is one of the intrinsic properties for the inorganic reagents as listed in Table 3. By using these λ and ΔG°, we estimated the "nuclear factor" in the ET reactions here (Table 3). To compare the nuclear factors for the ET reactions, we calculate the relative value of the nuclear factor, where the nuclear factor for the ET reaction with $Fe(CN)_6^{3-}$ is set to be 1. The nuclear factors for the ET reactions with the anionic acceptors are, at most, twice those of the cationic ones, while k_{ET} to the cationic acceptor is less than 10% of that to $Fe(CN)_6^{3-}$. Although λ and ΔG° have a large influence on the ET reaction in some ET reactions in proteins (*36*), the preferential ET to the anionic redox partner from ZnP450 cannot be attributed to the difference of the "nuclear factor" between the cationic and anionic redox partners.

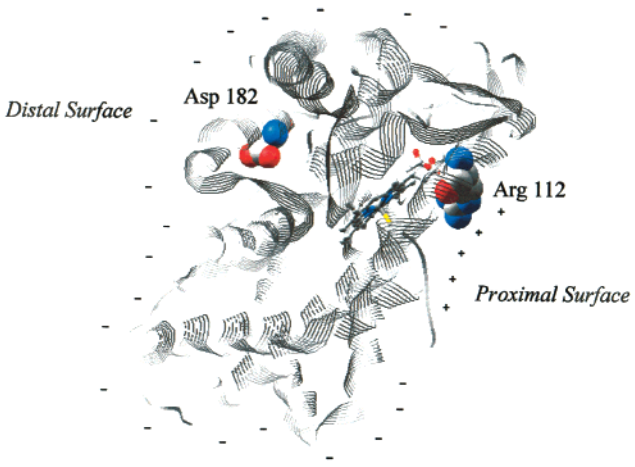

FIGURE 9: Schematic representation of the P450cam surface. The proximal face is closer to the heme, compared to the distal face. Data are taken from the 2.6 Å resolution crystal structure (ref *25*).

Since the remaining factor determining the ET reaction, the electronic factor, depends on the donor−acceptor distance (D−A distance), d, the preferential ET reaction to the anionic acceptor would be due to the short distance between zinc-porphyrin in ZnP450 and the anionic acceptor. Although the binding site of the inorganic compounds on the protein surface of P450cam is not clear, it would be rational that the negatively charged acceptor binds to the positive patch on the protein surface and the negatively charged protein surface is a good interaction site for the cationic acceptor. The closest positively charged residue to the heme iron on the proximal surface is Arg112 (9.3 Å), while the closest negatively charged residue on the distal surface is Asp182 (15.7 Å) (Figure 9). As estimated by the Marcus equation (eq 5), the ET rate with 9.3 Å D−A distance would be ca. 8.0×10^3-fold faster than that with 15.7 Å D−A distance under the same condition. Since the observed ET rate constant for 100-fold excess $Fe(CN)_6^{3-}$ without KCl was 1.0×10^5 s^{-1}, the longer D−A distance for the ET to $Co(phen)_3^{3+}$ is estimated as less than 10^2 s^{-1}, which is smaller than the phosphorescence decay rate constant, k_d, of ^{3}ZnP450* (6.2×10^2 s^{-1}). Thus, the preferential ET reaction to the anionic acceptor in ZnP450 can be interpreted as the difference of the D−A distance: the short D−A distance in the ET complex for the anionic acceptor induced the ET reaction from ^{3}ZnP450*, while the longer D−A distance for the cationic acceptor retards the ET reaction rate less than the phosphorescence decay rate, resulting in no observable ET reactions.

Reactions with Pd: Biological Implications. Although ZnP450 can transfer one electron to the inorganic acceptor by illumination of the laser, the ET reaction between ^{3}ZnP450* and Pd^{ox} was not observed even with 10-fold molar excess of Pd^{ox} over ZnP450. This is a rather unexpected result because the protein surface of Pd is dominated by negatively

charged amino acid residues (*35*) and Pd^{ox} can bind with ^{3}ZnP450* to form a complex ($K_A = 1.76 \times 10^{-2}$ μM^{-1}, Figure 8). Although ferric P450cam binds to Pd^{red} with higher K_A (6.3×10^{-1} μM^{-1}) (*39*) in the native P450-catalyzed monooxygenation reaction and the direction of the ET reaction from ZnP450 to Pd^{ox} is opposite to the enzymatic case, ferrous P450cam, which has the same charge as ZnP450, can also transfer an electron to Pd^{ox} ($27\ s^{-1}$) after specific complex formation under a similar K_A (1.10×10^{-2} μM^{-1}) to that in ^{3}ZnP450*/Pd^{ox} (*39*, *40*). Moreover, the redox potential difference in the ^{3}ZnP450*/Pd^{ox} complex (ca. 0.7 eV)[4] is much larger than that in the ferrous P450cam/Pd^{ox} complex (*41*) (ca. 0.05 eV), indicating that the ET reaction in the ^{3}ZnP450*/Pd^{ox} complex is thermodynamically feasible.

Under the assumption that λ is 1.0 to ~2.0 eV as found for the various protein−protein ET reactions (*30*) and that the D−A distance was 12 Å as estimated by the computer simulation (*7*), the Marcus equation (eq 5) predicts that the ET rate constant in the ^{3}ZnP450*/Pd^{ox} complex is ca. 8.4×10^4 ($\lambda = 1.0$ eV) to ~5.6×10^6 s^{-1} ($\lambda = 2.0$ eV). This predicted ET rate constant is much faster than the phosphorescence decay rate constant of ^{3}ZnP450* (6.2×10^2 s^{-1}),[5] allowing the ET reaction from ^{3}ZnP450* to Pd. However, no ET reaction was observed for the ^{3}ZnP450*/Pd^{ox} complex, showing that the actual ET rate constant would be less than 6.2×10^2 s^{-1} in the complex. These results suggest that the ET reaction between ^{3}ZnP450* and Pd cannot be explained by the Marcus theory under the conditions we assumed here.

Based on the Marcus equation (eq 5), a D−A distance of more than 16 Å ($\lambda = 1.0$ to ~2.0 eV, $\Delta G° = -0.7$ eV) would inhibit the ET reaction in the complex, while the D−A distance for the ET reaction between P450cam and Pd is at most 12 Å (*7*). One of the possibilities would be that the interaction between ^{3}ZnP450* and Pd^{ox} is different from that of the native ferric P450cam/Pd^{red} complex and the binding site of Pd on ^{3}ZnP450* is far from the heme moiety, compared to that in native P450cam. The binding site of Pd on ^{3}ZnP450* would be perturbed by the metal substitution, resulting in the longer (>16 Å) D−A distance than native P450cam/Pd complex in the ZnP450/Pd complex.

Another possible interpretation for no ET reaction to Pd would be that the conformational changes to facilitate the ET to Pd are not induced in ZnP450. As previously suggested (*42*), only one or a few conformers in the multiple conformers of the ET complex would contribute to the effective ET between P450cam and Pd, which has been referred to as the "conformational gating of ET in the P450cam/Pd complexes". Evidence of the conformational changes evoked by the binding of Pd has been provided by several studies (*43*, *44*). For example, resonance Raman studies (*44*) have shown that the stretching mode of the heme axial ligand, ν_{Fe-S}, in P450cam upshifts by ~3 cm^{-1} from 350.5 cm^{-1} upon the binding of Pd. In ZnP450, some conformational changes essential for the ET reaction by binding of Pd might be inhibited by the metal substitution and/or the opposite direction of the ET reaction. To reveal the plausible effects of conformational changes on the ET reaction in more detail, we are currently investigating the dependence of the ET rate constants in the P450cam/Pd complex on the solvent viscosity, which can perturb the protein conformational changes.

In summary, this study shows that only the positively charged patches on the P450cam surface are available for the efficient ET reactions with its redox partner due to the closer D−A distance. Therefore, we propose that the asymmetric charge distribution on P450cam is crucial for the regulation of the ET reactions. In the case of the reaction with Pd, however, some protein conformational changes would be required to transfer electrons between P450cam and Pd.

[4] We assume in this paper that an electron is transferred from ^{3}ZnP450* to Pd after ZnP450−Pd complex formation, and the redox potential of the P450cam-bound Pd (−0.20 eV), which is 0.04 eV higher than that of the free form of Pd (−0.24 eV) (*41*), was used for the estimation of the redox potential difference in ^{3}ZnP450*/Pd^{ox}.

[5] Even if the redox potential of the free form of Pd (−0.24 eV) is used, the estimated redox potential difference in ^{3}ZnP450*/Pd^{ox} is about 0.66 eV, which still corresponds to a much faster ET rate [ca. 6.5×10^4 ($\lambda = 1.0$ eV) to ~3.3×10^6 s^{-1} ($\lambda = 2.0$ eV)] than the phosphorescence decay rate of ^{3}ZnP450*.

ACKNOWLEDGMENT

We are grateful to Prof. Yuzuru Ishimura (Keio University) for a gift of the expression vector of the cytochrome P450cam gene. We are greatly indebted to Dr. Shigeo Umetani for the ICP measurement and Dr. Hiroshi Hori for the ESR measurement. We are also obligated to Dr. Satoshi Takahashi for the fruitful discussions.

REFERENCES

1. Mueller, E. J., Loida, P. J., and Sligar, S. G. (1995) in *Cytochrome P450: Structure, Mechanism, and Biochemistry* (Oritz de Montellano, P. R., Ed.) pp 83−124, Plenum Press, New York.
2. Stayton, P. S., Poulos, T. L., and Sligar, S. G. (1989) *Biochemistry 28*, 8201−8205.
3. Stayton, P. S., and Sligar, S. G. (1990) *Biochemistry 29*, 7381−7386.
4. Unno, M., Shimada, H., Toba, Y., Makino, R., and Ishimura, Y. (1996) *J. Biol. Chem. 271*, 17869−17874.
5. Holden, M., Mayhew, M., Bunk, D., Roitberg, A., and Vilker, V. (1997) *J. Biol. Chem. 272*, 21720−21725.
6. Aoki, M., Ishimori, K., and Morishima, I. (1998) *Biochim. Biophys. Acta 1386*, 157−167.
7. Pochapsky, T. C., Lyons, T. A., Kazanis, S., Arakaki, T., and Ratnaswamy, G. (1996) *Biochimie 78*, 723−733.
8. Roitberg, A. E., Holden, M. J., Mayhew, M. P., Kurnikov, I. V., Beratan, D. N., and Vilker, V. L. (1998) *J. Am. Chem. Soc. 120*, 8927−8932.
9. Vidakovic, M., and Germanas, J. P. (1996) *Protein Sci. 5*, 1793−1799.
10. Cheddar, G., Meyer, T. E., Cusanovich, M. A., Stout, C. D., and Tollin, G. (1989) *Biochemistry 28*, 6318−6322.
11. Christensen, H. E. M., Ulstrup, J., and Sykes, A. G. (1990) *Biochim. Biophys. Acta 1039*, 94−102.
12. Brunschwig, B. S., Delaive, P. J., English, A. M., Goldberg, M., Gray, H. B., Mayo, S. L., and Sutin, N. (1985) *Inorg. Chem. 24*, 3743−3749.
13. Butler, J., Chapman, S. K., Davies, D. M., Sykes, A. G., Speck, S. H., Osheroff, N., and Margoliash, E. (1983) *J. Biol. Chem. 258*, 6400−6404.
14. Adzamli, I. K., Petrou, A., Sykes, A. G., Rao, K. K., and Hall, D. O. (1983) *Biochem. J. 211*, 219−226.
15. Miyazaki, G., Morimoto, H., Yun, K., Park, S., Nakagawa, A., Minagawa, H., and Shibayama, N. (1999) *J. Mol. Biol. 292*, 1121−1136.
16. Ye, S., Shen, C., Cotton, T. M., and Kostic, N. M. (1997) *J. Inorg. Biochem. 65*, 219−226.
17. Gunsalus, I. C., and Wagner, G. C. (1978) *Methods Enzymol. 52*, 166−188.

18. Wagner, G. C., Perez, M., Toscano, W. A., Jr., and Gunsauls, I. C. (1981) *J. Biol. Chem. 256*, 6262−6265.
19. Greenfield, N., and Fasman, G. D. (1969) *Biochemistry 8*, 4108−4116.
20. Orii, Y. (1984) *J. Biol. Chem. 259*, 7187−7190.
21. Cheng, J., Zhou, J. S., and Kostic, N. M. (1994) *Inorg. Chem. 33*, 1600−1606.
22. Papp, S., Vanderkooi, J. M., Owen, C. S., Holtom, G. R., and Phillips, C. M. (1990) *Biophys. J. 58*, 177−186.
23. Anni, H., Vanderkooi, J. M., and Mayne, L. (1995) *Biochemistry 34*, 5744−5753.
24. Nappa, M., and Valentine, J. S. (1978) *J. Am. Chem. Soc. 100*, 5075−5080.
25. Poulos, T. L., Finzel, B. C., Gunsalus, I. C., and Wagner, G. C. (1985) *J. Biol. Chem. 260*, 16122.
26. Zemel, H., and Hoffman, B. M. (1981) *J. Am. Chem. Soc. 103*, 1192−1201.
27. Cowan, J. A., and Gray, H. B. (1989) *Inorg. Chem. 28*, 2074−2078.
28. Magner, E., and McLendon, G. (1989) *J. Phys. Chem. 93*, 7130−7134.
29. Peterson-Kennedy, S. E., McGourty, J. L., Kalweit, J. A., and Hoffman, B. M. (1986) *J. Am. Chem. Soc. 108*, 1739−1746.
30. Winkler, J. R., and Gray, H. B. (1992) *Chem. Rev. 92*, 369−379.
31. McLendon, G., and Miller, J. R. (1985) *J. Am. Chem. Soc. 107*, 7811−7816.
32. Hayashi, Y., and Yamazaki, I. (1979) *J. Biol. Chem. 254*, 9101−9106.
33. Kaneko, Y., Tamura, M., and Yamazaki, I. (1980) *Biochemistry 19*, 5795−5799.
34. Fuhrhop, J.-H., and Mauzerall, D. (1969) *J. Am. Chem. Soc. 91*, 4174−4181.
35. Pochapsky, T. C., Jain, N. U., Kuti, M., Lyons, T. A., and Heymont, J. (1999) *Biochemistry 38*.
36. Marcus, R. A., and Sutin, N. (1985) *Biochim. Biophys. Acta 811*, 265−322.
37. Wherland, S., and Gray, H. B. (1976) *Proc. Natl. Acad. Sci. U.S.A. 73*, 2950−2954.
38. (1984) *Handbook of Chemistry* (Ebihara, K., Ed.) Vol. II, Japanese Society of Chemistry, Tokyo.
39. Davies, M. D., and Sligar, S. G. (1992) *Biochemistry 31*, 11383−11389.
40. Mouro, C., Bondon, A., Jung, C., Hui Bon Hoa, G., De Certaines, J. D., Spencer, R. G. S., and Simonneaux, G. (1999) *FEBS Lett. 455*, 302−306.
41. Sligar, S. G., and Gunsalus, I. C. (1976) *Proc. Natl. Acad. Sci. U.S.A. 73*, 1078−1082.
42. Aoki, M., Ishimori, K., and Morishima, I. (1998) *Biochim. Biophys. Acta 1386*, 168−178.
43. Shimada, H., Nagano, S., Ariga, Y., Unno, M., Egawa, T., Hishiki, T., Masuya, F., Obata, T., and Hori, H. (1999) *J. Biol. Chem. 274*, 9363−9369.
44. Unno, M., Christian, J. F., Benson, D. E., Gerber, N. C., Sligar, S. G., and Champion, P. M. (1997) *J. Am. Chem. Soc. 119*, 6614−6620.

BI000874Y